

Influences of climate change on California and Nevada regions revealed by a high-resolution dynamical downscaling study

Lin-Lin Pan · Shu-Hua Chen · Dan Cayan ·
Mei-Ying Lin · Quinn Hart · Ming-Hua Zhang ·
Yubao Liu · Jianzhong Wang

Received: 4 April 2010 / Accepted: 25 November 2010 / Published online: 14 December 2010
© The Author(s) 2010. This article is published with open access at Springerlink.com

Abstract In this study, the influence of climate change to California and Nevada regions was investigated through high-resolution (4-km grid spacing) dynamical downscaling using the WRF (Weather Research & Forecasting) model. The dynamical downscaling was performed to both the GFS (Global forecast model) reanalysis (called GFS-WRF runs) from 2000–2006 and PCM (Parallel Climate Model) simulations (called PCM-WRF runs) from 1997–2006 and 2047–2056. The downscaling results were first validated by comparing current model outputs with the observational analysis PRISM (Parameter-elevation Regressions on Independent Slopes Model) dataset. In general, the dominant features from GFS-WRF runs and PCM-WRF runs were consistent with each other, as well as with PRISM results. The influences of climate change on the California and Nevada regions can be inferred from the

model future runs. The averaged temperature showed a positive trend in the future, as in other studies. The temperature increases by around 1–2°C under the assumption of business as usual over 50 years. This leads to an upward shifting of the freezing level (the contour line of 0°C temperature) and more rain instead of snow in winter (December, January, and February). More hot days (>32.2°C or 90°F) and extreme hot days (>37.8°C or 100°F) are predicted in the Sacramento Valley and the southern parts of California and Nevada during summer (June, July, and August). More precipitation is predicted in northern California but not in southern California. Rainfall frequency slightly increases in the coast regions, but not in the inland area. No obvious trend of the surface wind was indicated. The probability distribution functions (PDF) of daily temperature, wind and precipitation for California and Nevada showed no significant change in shape in either winter or summer. The spatial distributions of precipitation frequency from GFS-WRF and PCM-WRF were highly correlated ($r = 0.83$). However, overall positive shifts were seen in the temperature field; increases of 2°C for California and 3°C for Nevada in summer and 2.5°C for California and 1.5°C for Nevada in winter. The PDFs predicted higher precipitation in winter and lower precipitation in the summer for both California and Nevada.

L.-L. Pan · S.-H. Chen (✉) · Q. Hart · M.-H. Zhang
Department of Land, Air and Water Resources,
University of California, One Shields Avenue,
Davis, CA 95616, USA
e-mail: shachen@ucdavis.edu

L.-L. Pan · Y. Liu
Research Applications Laboratory,
National Center for Atmospheric Research, Boulder, CO, USA

D. Cayan
Scripps Institution of Oceanography,
University of California, San Diego, CA, USA

M.-Y. Lin
Taiwan Typhoon and Flood Research Institute,
Taichung, Taiwan

J. Wang
California Department of Water Resources,
Sacramento, CA, USA

1 Introduction

A warming of the climate has been observed globally and in the western United States (e.g., California and Nevada), mainly due to anthropogenic forcing (Intergovernmental Panel on Climate Change, IPCC 2007; U. S. Global Change Research Program 2009). Climate-related changes include increased surface air temperature and atmospheric

water vapor, more severe weather extremes, changes in precipitation patterns and intensity, more common and intense floods and droughts, reduced snowpack, earlier melting of the snowpack, shifting of the runoff timing, and a rise in sea level (e.g., IPCC 2007). Climate change will stress water resources, impact energy supply and demand, challenge crop and livestock production, increase risk to human health, and affect the environment and ecosystems.

Trenberth et al. (2007) showed that the global mean surface air temperature has risen around 0.74°C over the last 100 years (1906–2005), and the rate of increase has accelerated from $0.07^{\circ}\text{C}/\text{decade}$ over the last 100 years to $0.13^{\circ}\text{C}/\text{decade}$ over the last 50 years. Surface air temperatures have increased more over land ($0.27^{\circ}\text{C}/\text{decade}$) than over ocean ($0.13^{\circ}\text{C}/\text{decade}$). Therefore, increases in the frequency of extreme high average temperatures are expected (Easterling et al. 2000; DeGaetano and Allen 2002; Meehl and Tebaldi 2004). As the result of rising temperature, more precipitation falls as rain instead of snow for locations and seasons with climatological mean temperatures around 0°C . Observational studies have shown an earlier onset of spring and longer liquid precipitation seasons in some high latitude regions in the last 50 years (Cayan et al. 2001; Groisman et al. 2001, 2005, 2007; Easterling 2002).

Increasing air temperature also increases the water holding capacity of the atmosphere. Increased temperatures have raised water vapor over oceans by about 5% over the last century for the same relative humidity (e.g., IPCC 2007). More moisture in the atmosphere has generally increased precipitation intensity and the risk of heavy rain and snow events. The events of heavy (upper 5%) and very heavy (upper 1%) precipitation have increased by 14 and 20%, respectively, in the U.S. during the last three decades of the twentieth century, especially over the eastern parts of the country (Kunkel et al. 2003; Groisman et al. 2004). However, the total precipitation and/or the frequency of days with an appreciable amount of precipitation (wet days) may be unchanged or decreasing (Easterling et al. 2000; Sun and Groisman 2004; Groisman et al. 2005; Im et al. 2009). It was also reported that there has been an increase in both severe droughts and heavy rains in many regions of the world (Huntington 2006; Allan and Soden 2008; Kendon et al. 2008). The variation of precipitation in the second half of the twentieth century was dominated by variations on interannual to inter-decadal time scales (Manton et al. 2001; Peterson et al. 2002; Griffiths et al. 2003; Herath and Ratnayake 2004).

Some studies have focused on the influence of climate change on the western United States (Dettinger and Cayan 1995; Cayan 1996; Leung and Ghan 1999; Barnett et al. 2004, 2008; Dettinger et al. 2004; Leung et al. 2004; Pierce et al. 2008; Mote and Salathé 2010). Results show the snow

water equivalent (SWE) for the western U.S., as measured on April 1, has decreased from 1950 (60 cm; Mote 2003) to 2000 (50 cm), except in the southern Sierra Nevada (Mote 2003, 2006; Vanrheenen et al. 2004; Mote et al. 2005). More winter precipitation fell as rain instead of snow in the period 1949–2004 (Knowles et al. 2006), and earlier snowmelt runoff was also observed (Dettinger and Cayan 1995; Cayan et al. 2001; Stewart et al. 2004; Rauscher et al. 2008). Moreover, warming trends of the minimum daily temperatures over western and central North America were observed (Robeson 2004). Precipitation has generally increased during the winter and spring, the wettest seasons in states such as California and Nevada, over the past 50 years, while summer and fall have decreased in precipitation (NOAA's National Climatic Data Center 2008; U. S. Global Change Research Program 2009). A more arid climate in the southwestern part of the North America is predicted (Seager et al. 2007). However, there are still some debates on how the precipitation pattern will change for these regions in the future (e.g., Weare 2008).

Dynamically downscaling from coarse-resolution global-model simulations to higher-resolution regional-scale outputs has been conducted in previous studies (e.g., Jones et al. 1997; Christensen et al. 1998; Giorgi and Shields 1999; Leung and Ghan 1999; Small et al. 1999; Snyder et al. 2004; Kim et al. 2002; Bell et al. 2004; Leung et al. 2004; Kanamitsu and Kanamaru 2007; Caldwell et al. 2009). However, most of these studies (e.g., Bell et al. 2004; Leung et al. 2004; Caldwell et al. 2009) used a relatively coarse resolution (e.g., about 10–40 km), which is not sufficient to study climatic changes at regional scales in mountainous regions, such as the Sierra Nevada. Therefore, higher resolution (4 km) dynamical-scaling simulations over California and Nevada regions were carried out here.

In this study we refined our understanding of regional changes in California and Nevada, especially those related to precipitation and extreme events (e.g., heat waves, heavy precipitation), through WRF (Weather Research Forecast) model dynamical downscaling. The model and data are described in Sect. 2, followed by a comparison between the dynamical downscaling results and statistical downscaling results in Sect. 3. The influence of climate change on California and Nevada is discussed in Sect. 4. A summary and conclusions are given in Sect. 5.

2 Description of model, data, and experiment design

2.1 Model

The Weather Research and Forecasting (WRF) Model, a community-developed mesoscale model, was used to dynamically downscale the global model outputs, including

Global Forecast System (GFS) reanalysis and Parallel Climate Model (PCM) simulations, to finer resolution in the California and Nevada region. PCM can capture ENSO (El-Niño Southern Oscillation) and PDO (Pacific Decadal Oscillation) dominant features very well (e.g., Joseph and Nigam 2006; Meehl and Hu 2006). As a mesoscale model, WRF can simulate the local response for a given ENSO or PDO environmental forcing. WRF is a compressible, non-hydrostatic model, using terrain-following coordinates and governing equations written in flux-form, which conserves mass and dry entropy. The Runge–Kutta third-order time scheme was used and the fifth and third-order advection schemes were chosen for the horizontal and vertical directions, respectively. The advanced research WRF (ARW) model version 2.2 (Skamarock et al. 2005) was adopted for all simulations.

2.2 Data

Future initial and boundary conditions were provided by PCM simulations under the business as usual (BAU) scenario. PCM is a coupled climate model. The atmospheric component is the National Center for Atmospheric Research (NCAR) Community Climate Model; the ocean component is the Parallel Ocean Program with 32 vertical

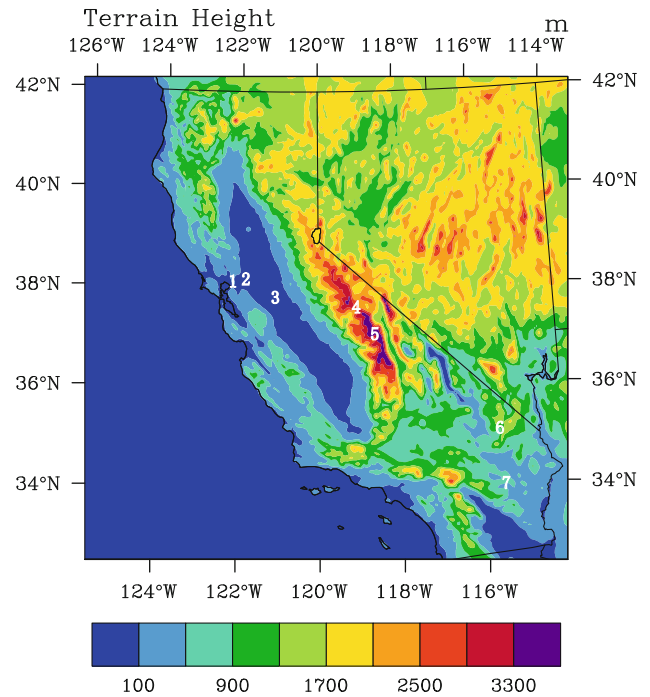
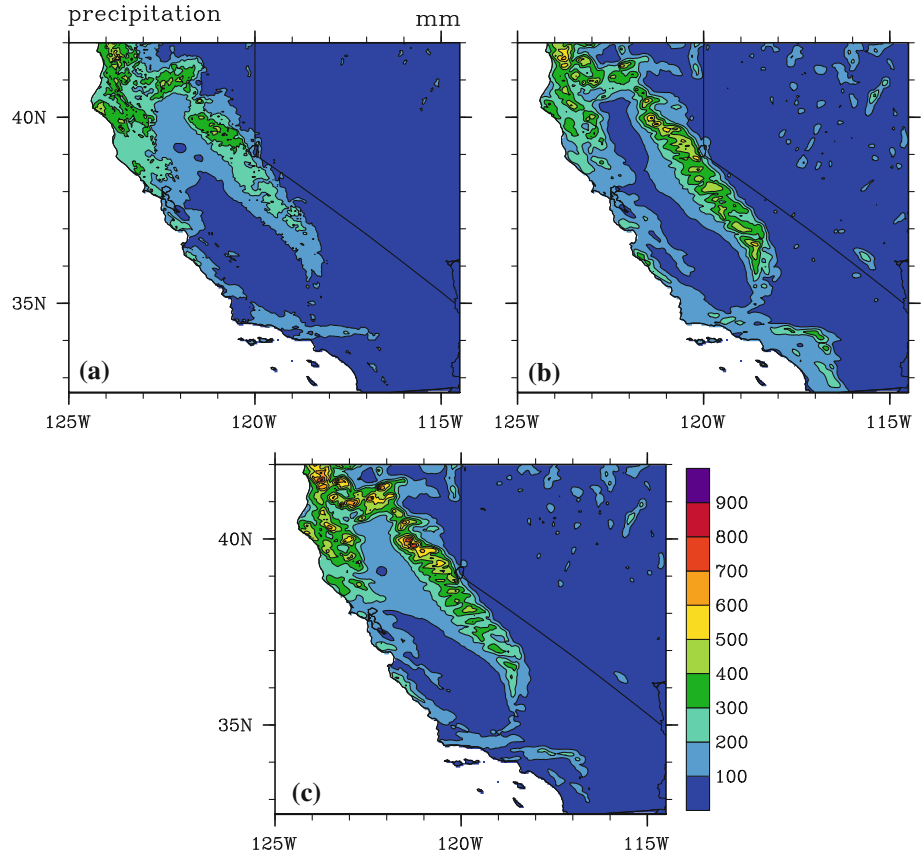


Fig. 2 Terrain of the model domain 3, where locations mentioned in the text are highlighted with: (1) Carquinez Strait, (2) Sacramento Delta, (3) Central Valley, (4) Sierra Nevada, (5) mountain ridge (higher elevation), (6) Mojave Desert, and (7) Palm Desert

Fig. 1 Monthly averaged precipitation (mm) during the winter season (i.e., December, January, and February) from 2000 to 2006 for **a** PRISM, **b** PCM-WRF outputs, and **c** GFS-WRF outputs



levels and a horizontal resolution of $2/3^\circ$. The sea ice component is the Naval Postgraduate School model using a resolution of 27 km. The horizontal resolution of PCM data used here was about $2.8^\circ \times 2.8^\circ$, and the time

interval for most of the PCM variables was 6 h. To validate the PCM data, current PCM data was downscaled and compared to downscaled GFS reanalysis data. GFS is a medium-range, global model. The horizontal resolution

Fig. 3 Differences of monthly averaged precipitation (mm) during the winter season from 2000 to 2006 **a** between PCM-WRF runs and PRISM, and **b** between GFS-WRF runs and PRISM

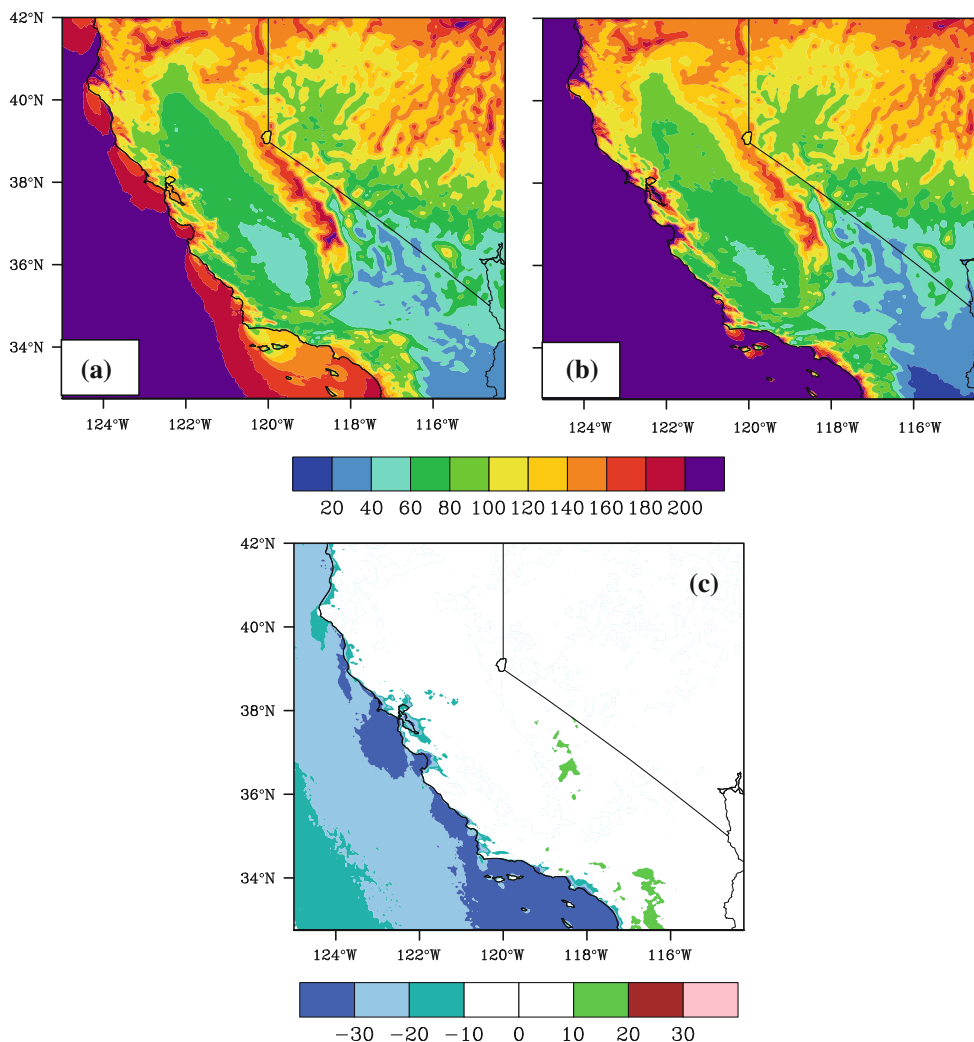
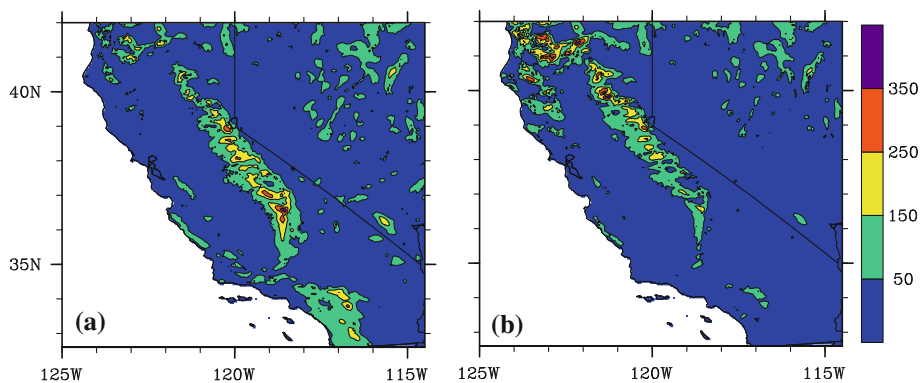


Fig. 4 Averaged yearly number of rainy days from 2000 to 2006 for **a** PCM-WRF runs, **b** GFS-WRF runs, and **c** their difference. The threshold for a rainy day is 1 mm

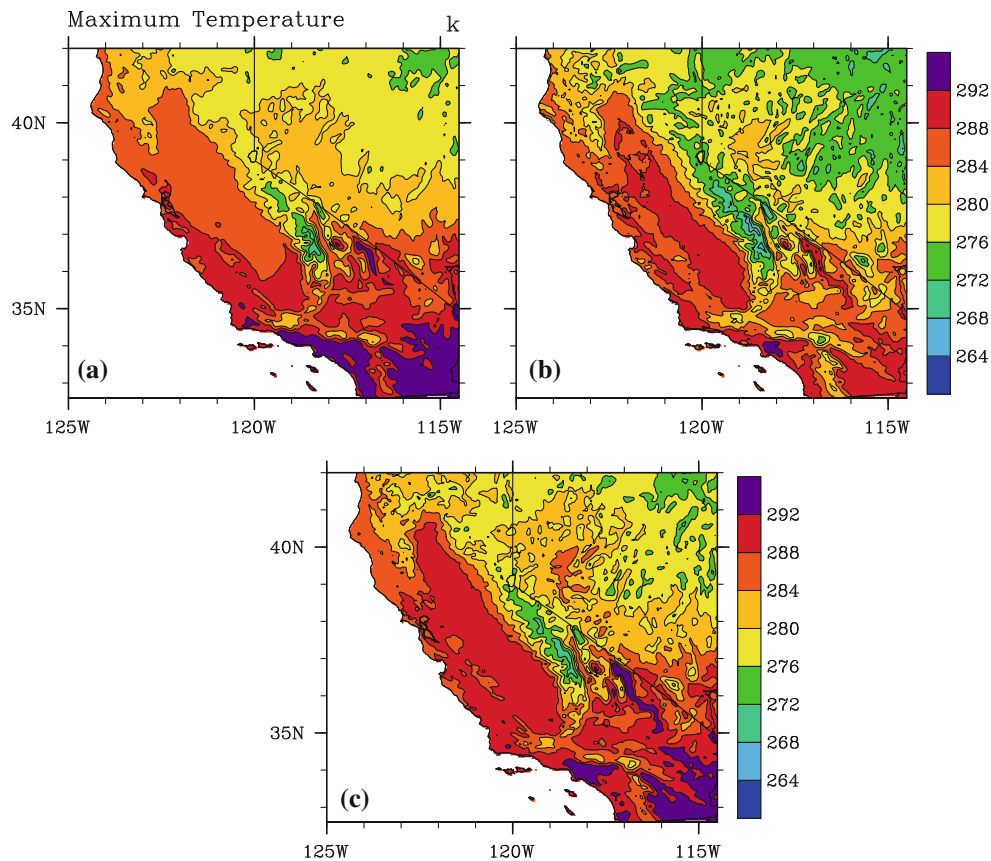


Fig. 5 Averaged daily maximum 2-m temperature (K) during the winter season from 2000 to 2006 for **a** PRISM, **b** PCM-WRF runs, and **c** GFS-WRF runs

of reanalysis is $1^\circ \times 1^\circ$ and the time interval of the data set is 6 h.

For dynamical downscaling, 7 years of GFS reanalysis (2000–2006) and 10 years of both current PCM climate simulations (1997–2006) and future PCM climate simulations (2047–2056) were used. Ten-year time periods of PCM data were chosen for climate study, as suggested by Jones et al. (1997). However, for GFS reanalysis, only 7 years data were used because the model resolution was upgraded from T126L28 to T170L42 (T refers to horizontal spectral truncations, L refers to vertical level) in 2000 (http://www.emc.ncep.noaa.gov/gmb/STATS/html/model_changes.html).

The dynamical downscaling results were also validated through comparison with the statistical downscaling results from PRISM (Parameter-elevation Regressions on Independent Slopes Model) (Daly et al. 1994; DiLuzio et al. 2008). PRISM data are gridded interpolations from station data based on weighting functions using distance, elevation, topographic facet, atmospheric layer, orographic effectiveness, and coastal proximity as parameters. Thus the spatial scale and pattern of each

variable (e.g., precipitation) are well preserved in PRISM, and the data can even be used in areas with complex terrain. PRISM data are available monthly with a horizontal resolution of 4 km, similar to the scale of dynamical downscaling simulations. The data period used here is from 1997 to 2006 (the same as the model time period).

2.3 Experimental design

For the downscaling, WRF simulations were run twice a month using GFS reanalysis or PCM outputs as initial and boundary conditions. Three domains with two-way interaction were simulated and the resolutions were 36 km, 12 km, and 4 km for domains 1–3, respectively. The numbers of grid points for domains 1, 2, and 3 were $91 \times 95 \times 31$, $145 \times 145 \times 31$ and $271 \times 310 \times 31$ points, respectively, in the x – y – z directions. The highest-resolution domain covers (33°N – 42°N , 125°W – 115°W). The Lambert projection was used in the model, which gives even grid spacing, unlike lat-lon coordinates. Four dimensional data assimilation (i.e., nudging; see Liu et al.

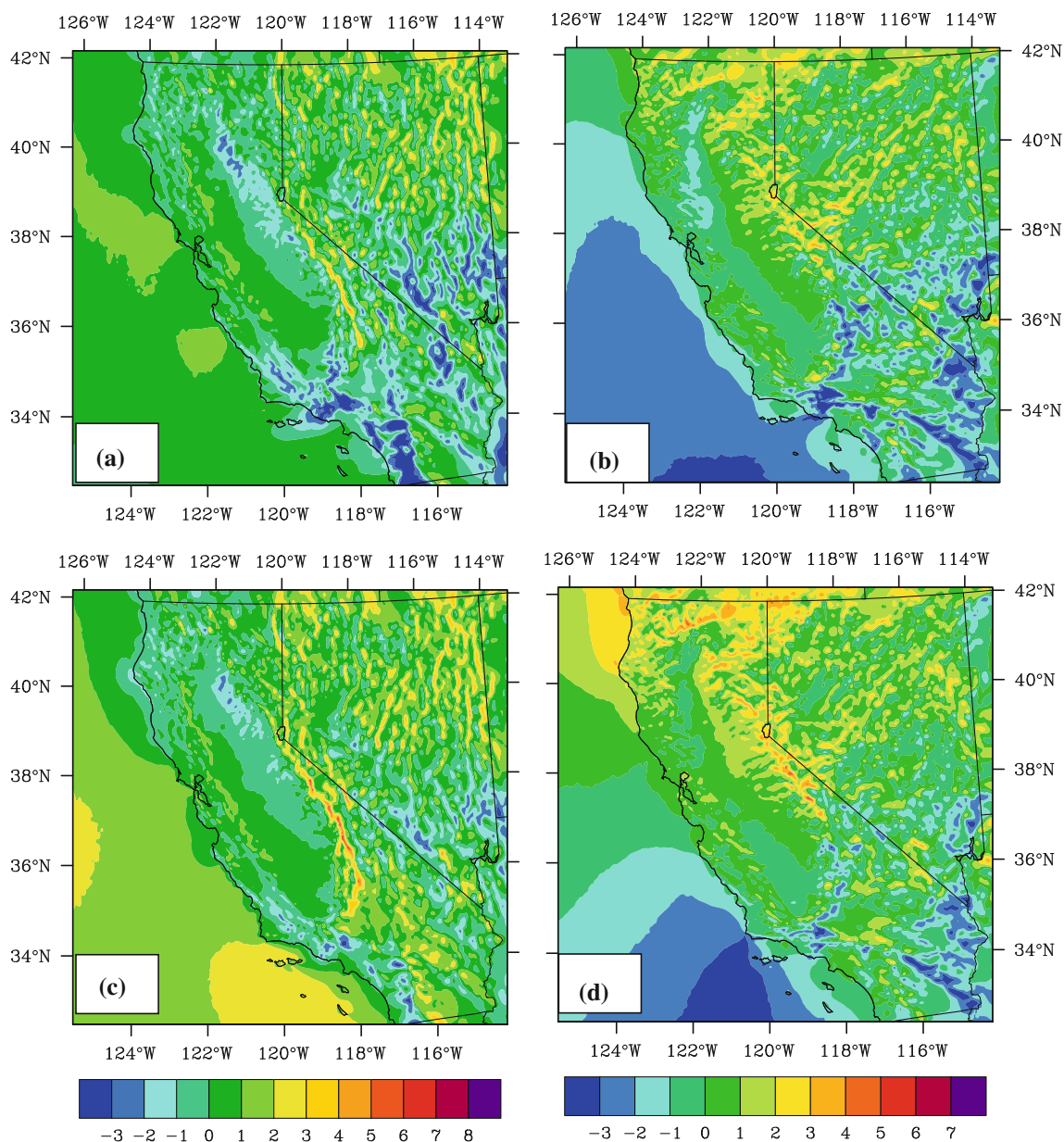


Fig. 6 Averaged **a** zonal wind and **b** meridional wind during the winter season from 2000 to 2006 for PCM-WRF runs. **c** and **d** are the same as **(a)** and **(b)**, except for GFS-WRF runs

2008 for details) was applied to domain 1 using PCM/GFS data to retain the large-scale properties from the global model simulations or reanalysis. The physics schemes that were used for simulations were Grell-Devenyi cumulus parameterization (Grell and Devenyi 2002), WRF Single-Moment 6-class (WSM6) cloud microphysics (Hong et al. 2004), Yonsei University (YSU) planetary boundary parameterization (Hong et al. 2006), Rapid Radiation Transfer Model long-wave radiation (Mlawer et al. 1997) and Dudhia short-wave radiation (Dudhia 1989). No cumulus parameterization was applied to domain 3 because

of its fine resolution. The model was integrated with a time step of 180 s for domain 1.

3 Comparison of the dynamical downscaling results with the statistical downscaling PRISM dataset

The dynamical downscaling results from GFS reanalysis (called GFS-WRF runs) and PCM simulations (called PCM-WRF runs) were compared with the statistical downscaling (PRISM) results. The variables investigated

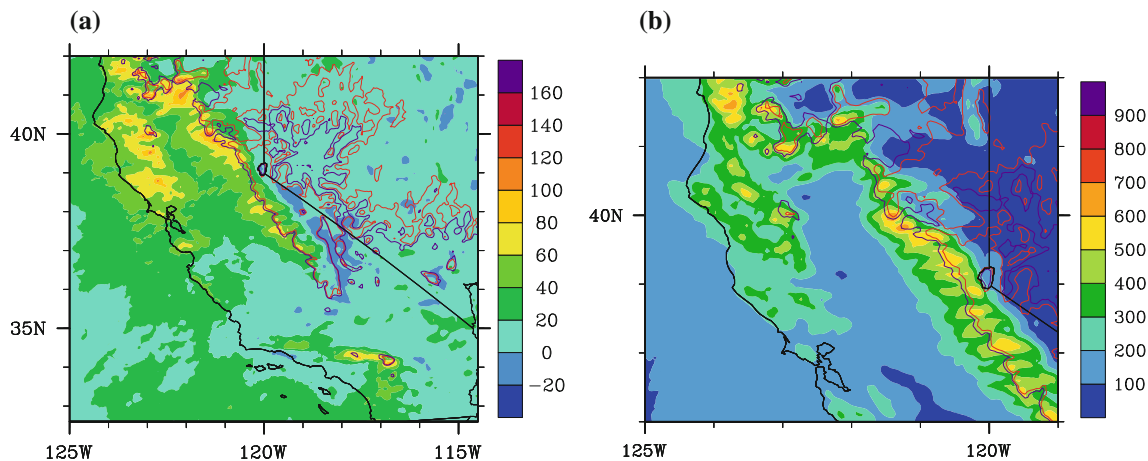


Fig. 7 **a** Difference of averaged monthly precipitation (mm) during the winter season between future PCM-WRF runs (2047–2056) and current PCM-WRF runs (1997–2006), future–current. The *red line* is the freezing line of future PCM-WRF runs during winter and the *purple line* is the freezing line of current PCM-WRF runs. **b** Averaged

monthly precipitation (mm) during the winter season for future PCM-WRF runs (2047–2056). The *red line* is the freezing line of future PCM-WRF runs during winter and the *purple line* is the freezing line of current PCM-WRF runs (1997–2006)

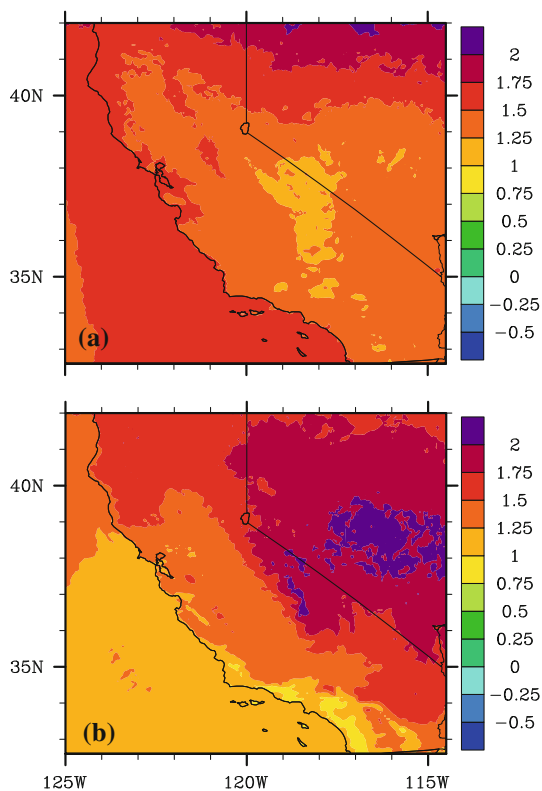


Fig. 8 Difference of averaged daily 2-m temperature (K) during the **a** winter and **b** summer seasons between future PCM-WRF runs (2047–2056) and current PCM-WRF runs (1997–2006), future–current

here include precipitation, the surface maximum and minimum temperature, and the surface wind field. Due to the shorter time period of data sets from GFS (i.e., 2000–2006), only results from 2000 to 2006 were used for

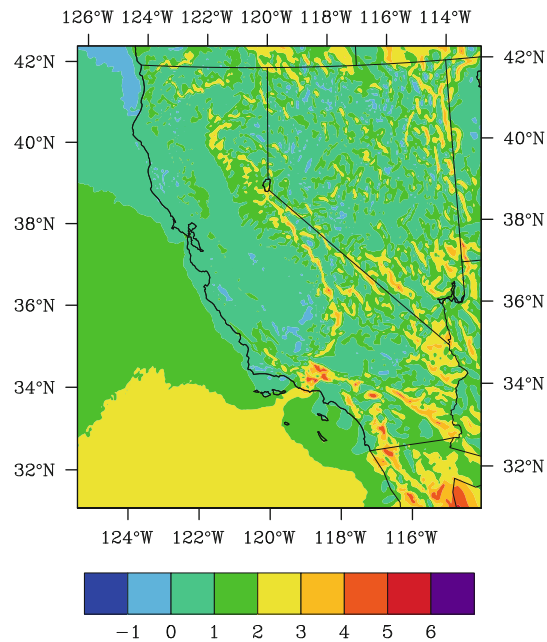


Fig. 9 Difference of averaged 10-m wind speed (m/s) during the winter season between future PCM-WRF runs (2047–2056) and current PCM-WRF runs (1997–2006), future–current

comparison among these three data sets (i.e., GFS-WRF, PCM-WRF, and PRISM).

3.1 Precipitation

The western U.S. has its maximum precipitation in winter and minimum in summer due to a north–south seasonal shift of the Pacific high and mid-latitude storm track. Topography also plays an important role in precipitation

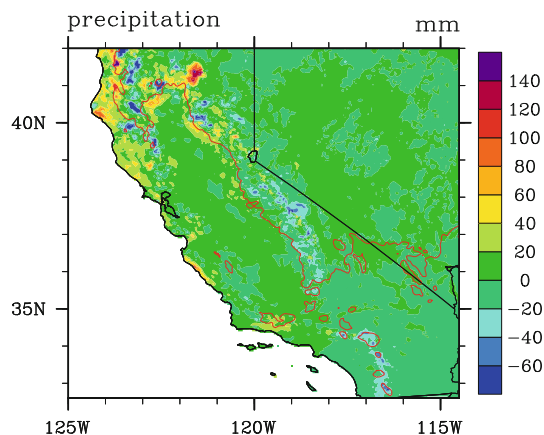


Fig. 10 Difference of monthly mean precipitation during the winter season between current (1999–2008) and past PRISM results (1979–1988), current–past, and the freezing line of current mean temperature from PRISM (1999–2008) (*red line*) during winter

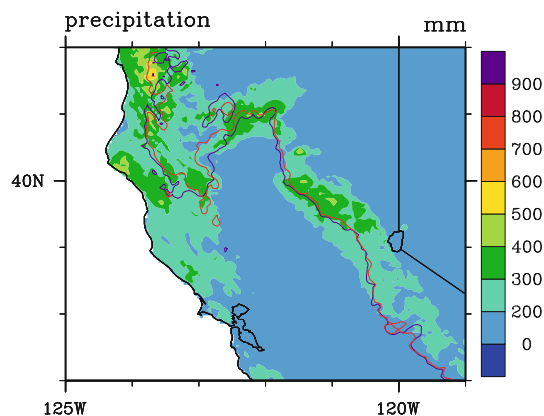


Fig. 11 Current (1999–2008) monthly mean precipitation from PRISM during the winter season and freezing line of the current (1999–2008, *red line*) and past PRISM (1979–1988, *purple line*) mean temperature during winter

patterns; mountain blocking and orographic lifting effects produce more precipitation on the windward sides of the mountain ranges. Snowmelt from winter snow stored in the Sierra Nevada mountain range provides the major water source for irrigation in the next growing season in CA (<http://www.wrcc.dri.edu/narratives/CALIFORNIA.htm>).

Dominant precipitation features for California were captured in both the WRF simulations and PRISM results (Fig. 1). Maximum precipitation occurred at the mountain tops (Fig. 2) with values around 500–600 mm/month for PRISM, 600–700 mm/month for PCM-WRF runs, and 700–800 mm/month for GFS-WRF runs. The maximum values simulated from the dynamical downscaling results were slightly larger than those from PRISM. Statistical downscaling may have difficulty extrapolating to higher elevations due to fewer available observations. The rainfall patterns of these three results were consistent except that

PCM-WRF runs had a slight wet bias (around 50 mm) in the southern part of California.

PCM-WRF precipitation predictions were not only larger than PRISM results, but also extended farther southward (Fig. 3a). The maximum difference between PCM-WRF and PRISM can vary from 150 mm/month to 250 mm/month (yellow area in the figure) at the mountaintop. The southward shift is not obvious in the GFS-WRF simulations (Fig. 3b), but they show more precipitation in higher elevations. The standard deviations of precipitation were calculated for PRISM, PCM-WRF, and GFS-WRF (not shown), which also have their maximum value of around 400 mm/month at the mountaintops. A large standard deviation implies large inter-annual variation in precipitation. The average annual number of precipitation days is shown in Fig. 4. The threshold for a rainy day is 1 mm. Results from PCM-WRF and GFS-WRF were highly correlated (the pattern correlation is around 0.83, and is significant at a 95% confidence level), with higher precipitation frequency over the oceans and at higher elevations. Compared to GFS-WRF runs, PCM-WRF runs produced more rainy dates over the southern Sierra Nevada and fewer rainy days over the ocean near the coastal region, particularly near the coast of southern CA.

3.2 Temperature

The dominant features of the averaged 2-m maximum and minimum air temperature fields from PRISM were reasonably captured by dynamical downscaling during the winter season. Compared with GFS-WRF runs, the values of the maximum 2-m temperature from PCM-WRF were closer to those from PRISM over the Central Valley, while those from GFS-WRF runs were around 1° closer than PCM-WRF modeled values to those from PRISM for the rest of domain 3 (Fig. 5). For averaged daily minimum temperature in winter (not shown), results from PCM-WRF were closer to PRISM than GFS-WRF results were. This is unexpected and requires further study (e.g., studying the data used in GFS/PCM simulation). GFS-WRF runs should have been closer to PRISM since actual observations were assimilated into GFS reanalysis. The analysis on diurnal and seasonal data also showed lower diurnal and seasonal variation of the temperature on the coast compared to inland regions due to the adjustment from the ocean (figure not shown). Higher elevations also experienced larger temperature variation.

3.3 Wind field

California is located in the path of the mid-latitude westerlies; the wind direction can be west, northwest or

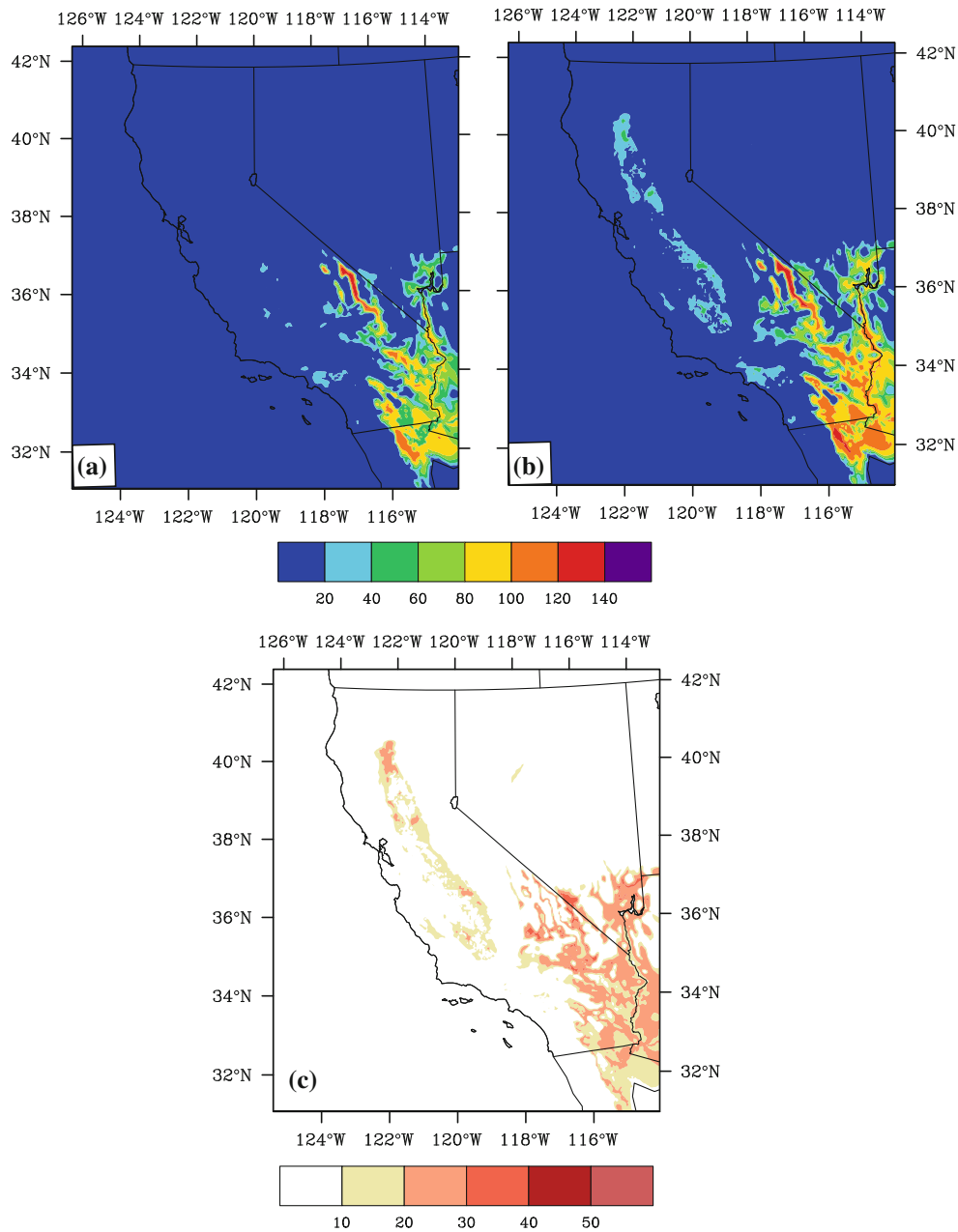


Fig. 12 Average number of extreme hot days (>100° F or 37.8°C) from PCM-WRF runs during the warm season (i.e., May to October) for **a** 1997–2006, **b** 2047–2056, and **c** their differences (future–current)

southwest over ocean. However, the inland wind field is very complex due to topographic effects (Fig. 6). PRISM does not contain wind field. Therefore, only the dynamical downscaling 10-m winds from PCM (Fig. 6a) and GFS (Fig. 6b) were compared. Overall, their dominant features were similar, except over parts of the ocean. However, winds over mountain ridges were higher from GFS-WRF runs than from PCM-WRF runs. For the zonal wind, most regions had positive values (westerly component) over ocean and mountain, and the maximum value was around 5–7 m/s at the mountain top; negative

values are found in the Sacramento Valley. For the meridional wind, negative values (northerly component) were found along the south part of the coast region. The northerly wind along the coast can produce oceanic upwelling due to Ekman pumping. The maximum value of meridional wind was around 4–6 m/s at higher elevations.

Overall, these experiments show that the dominant features of precipitation, temperature, and wind fields are well simulated by WRF runs using PCM based initial and boundary conditions. The magnitude, spatial pattern,

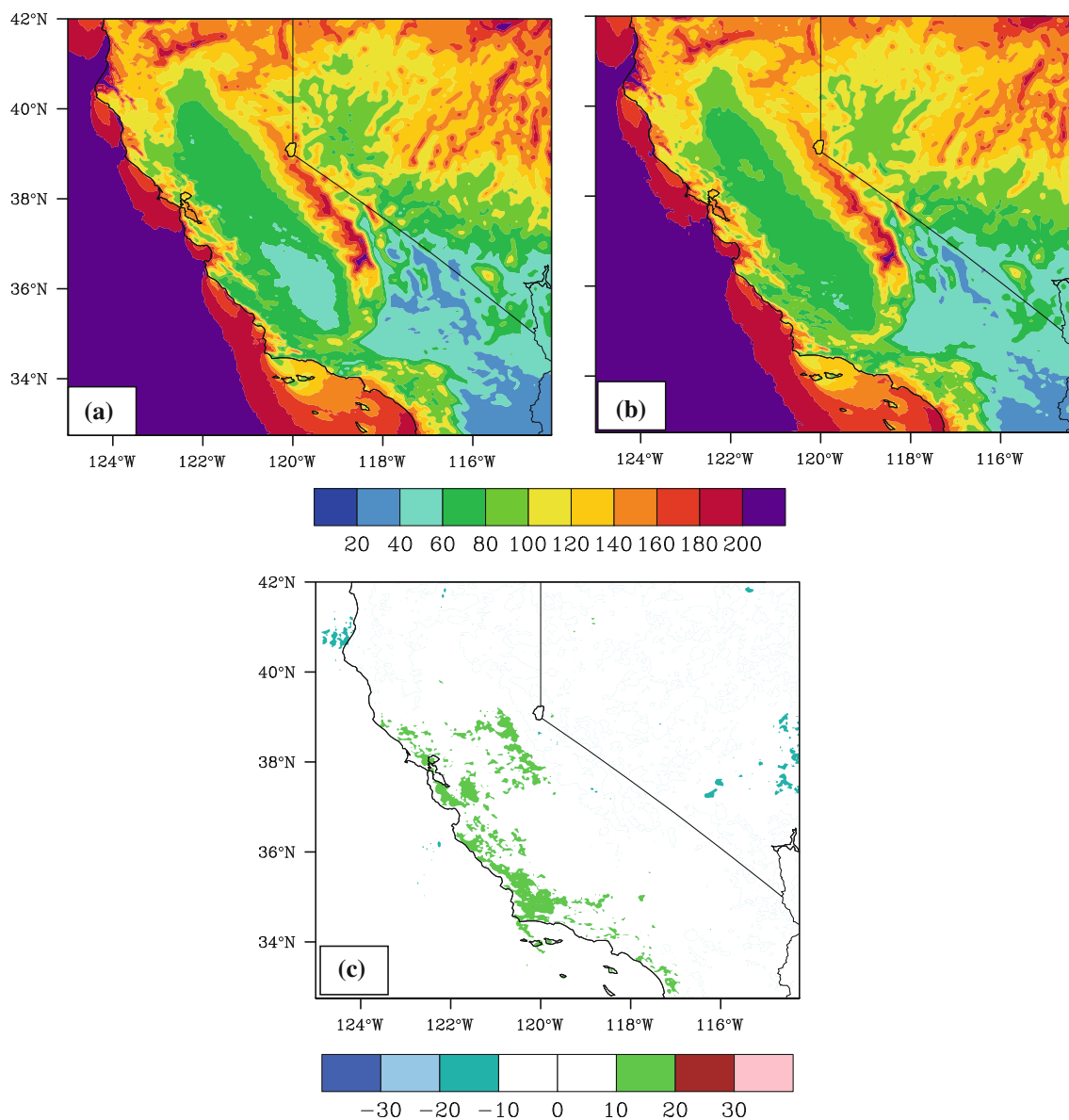


Fig. 13 Number of rain days (daily rainfall > 1 mm) for **a** current (1997–2006), **b** future (2047–2056), and **c** their difference (future–current)

and seasonal variations of these variables are well reproduced by PCM-WRF runs when comparing with the PRISM dataset and reanalysis results (GFS-WRF runs).

4 The potential influence of climate change on California

4.1 The influence of climate change to the mean fields

The influence of climate change on California can be predicted by comparing current and future meteorological fields. Comparison of WRF models using current

(1997–2006) and future (2047–2056) PCM inputs showed increases in both precipitation (Fig. 7a, b) and temperature (Fig. 8). An upward shift of the freezing level in the future climate was also predicted (Fig. 7a, b). Here, the freezing level is defined by the 0°C contour line of the mean 2-m temperature. More rainfall also occurred below the freezing level. Although more precipitation will occur in the future, more falls as rain and cannot be stored for summer use (US Climate Change research program 2009). The new snow pack predicted above the freezing level (i.e., gain of snow in the future) is approximately 15% less than the lost snow pack between the two freezing levels, (i.e., loss of snow in the future due to climate warming).

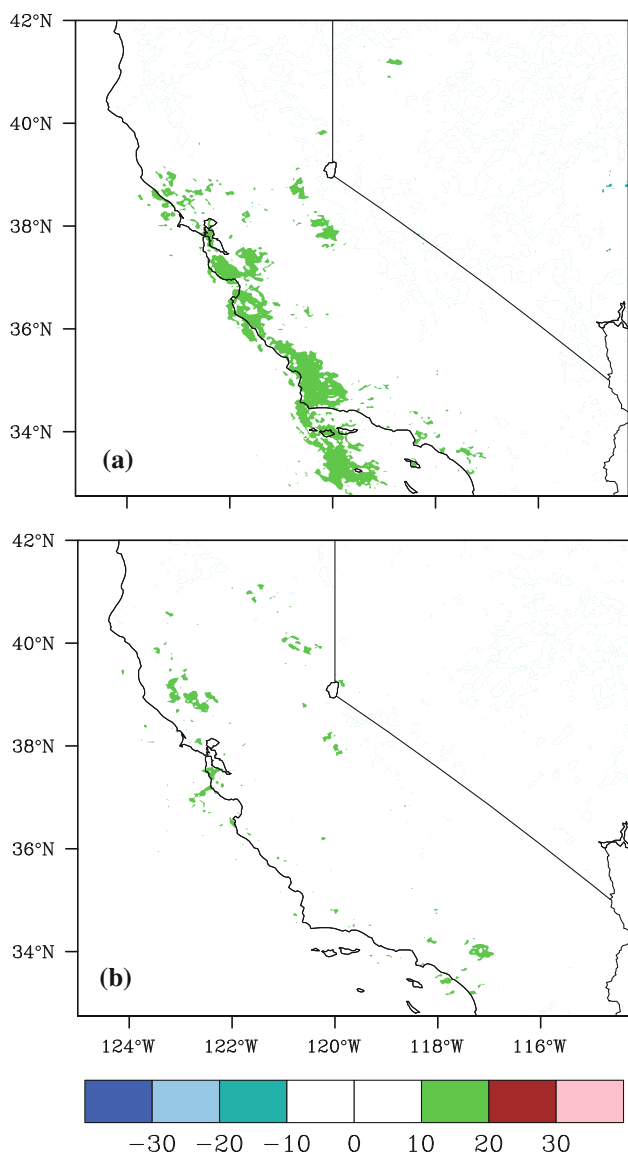


Fig. 14 Same as in Fig. 13c except for **a** daily rainfall > 10 mm, and **b** daily rainfall > 100 mm

Surface wind speed change is moderate, under 1–2 m/s in most of the region, though larger (>2 m/s) at ridge tops, in southern CA, and over the southern part of the ocean (Fig. 9).

The trend of climate change was also seen in PRISM data. Here trend is defined as an increasing or decreasing tendency in a climate variable's behavior over a specific period of time at a given place. An increasing (decreasing) tendency is called a positive (negative) trend (<http://www.nws.noaa.gov/climate/help/glossary.php>). Comparing current (1999–2008) and past meteorological fields (1979–1988) showed an increase in precipitation in some regions (Figs. 10, 11) (e.g., northern side of coast region) as well as changing freeze lines (Fig. 11).

4.2 Impact of climate change on extreme events in California and Nevada regions

The possible influence of climate change on extreme events (e.g., extreme hot days, heavy precipitation) in California and Nevada regions can also be inferred from the current and future WRF simulations. Both extreme hot days (>100°F or 37.8°C) (Fig. 12) and precipitation days (>1 mm/day) (Fig. 13) are expected to increase. More hot days are expected in the Central Valley and Mojave Desert (Fig. 12). Increases in precipitation events were mainly located in the coastal regions of central California (Fig. 13c). One possible reason is that increasing temperature will increase the capacity of atmospheric moisture acquisition over the ocean (IPCC 2007; U. S. Global Change Research Program 2009). The coastal region therefore receives more rainfall, with smaller moisture increases inland due to topographic blocking effects. However, around San Francisco, the moisture can intrude further inland by passing through the Carquinez Strait and cause increased rainfall on the Sacramento Delta. Medium rainfall events (daily precipitation > 10mm) change mostly in the coastal region (Fig. 14a), with heavy rainfall events (daily precipitation >100 mm) occurring more often in the Southern coast and the mountainous regions of northwestern California (Fig. 14b). This may relate to large-scale forcing (<http://www.wrcc.dri.edu/narratives/CALIFORNIA.htm>), e.g. cold fronts from the north or tropical storms from the south. However, the signal is weak, and further studies are needed.

4.3 Changing probability distribution functions (PDF) due to a warming climate

The changes in probability distribution functions of temperature, precipitation and wind speed due to climate change were further analyzed for California and Nevada. Based on hourly-averaged data, we obtained the grid-averaged 2-m temperature, precipitation, and 10-m wind speed for each of the states, and then performed a probability distribution analysis on the mean temperature, total precipitation, and mean wind speed for winter (Fig. 15) and summer (Fig. 16). The temperature probability distribution function (PDF) peak shifted 2.5°C and 1.5°C higher for winter, from current to future, for California and Nevada, respectively (Fig. 15a, b). The summer temperature shift in Nevada was around 3°C, larger than the 2.2°C shift of California (Fig. 16a, b). The warming in California is relatively greater in winter than in the summer, however, in Nevada this is reversed. Both California and Nevada are anticipated to have drier summers (Fig. 16c, d). In winter, California becomes wetter with heavier rainfall events, and there will be little change in Nevada, except that the PDF

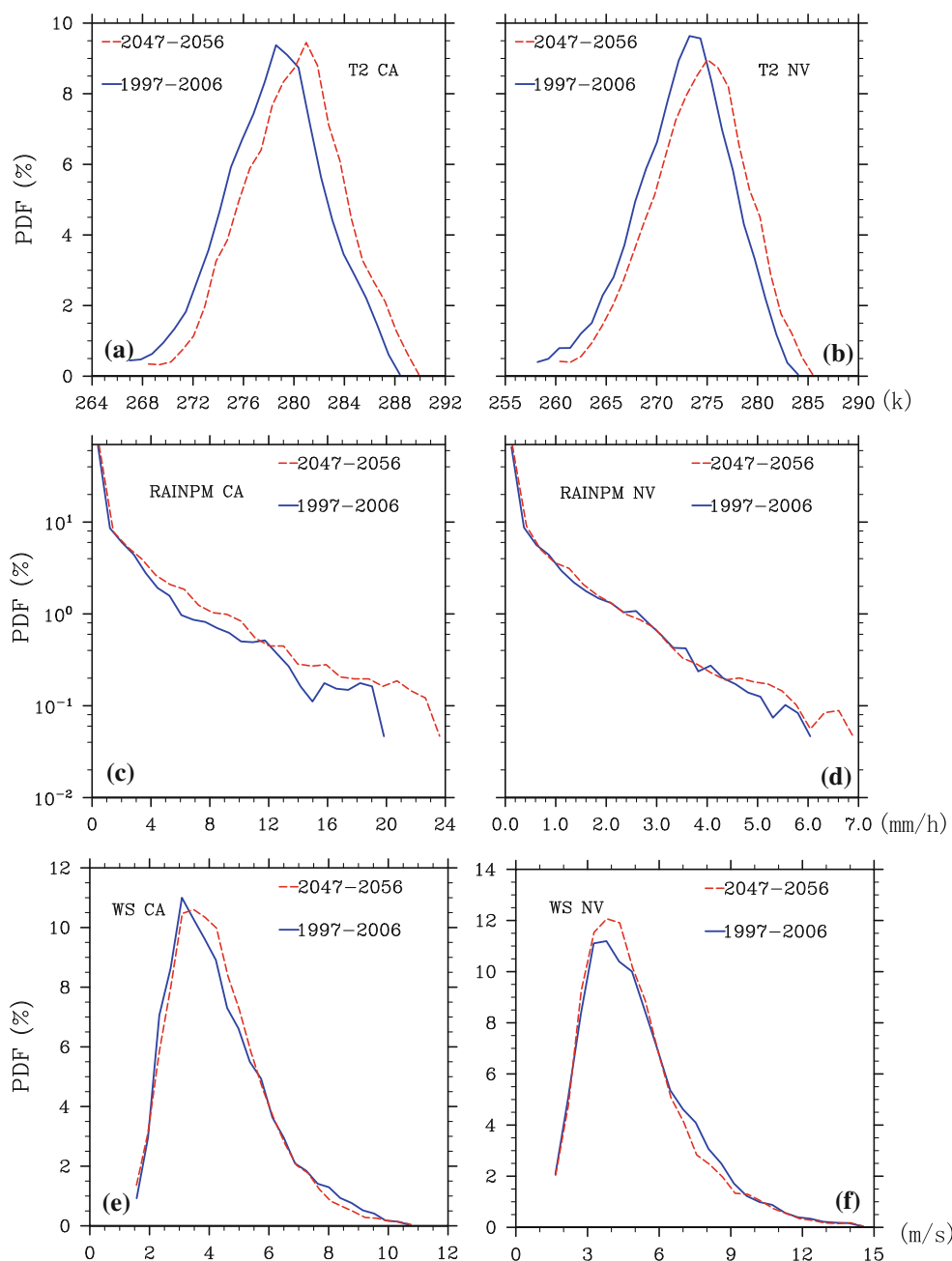


Fig. 15 Probability distribution function (PDF) for California (a, c, e) and Nevada regions (b, d, f) for temperature (a, b), rainfall (c, d), and wind speed (e, f) in winter. The units are K, mm per hour for the whole domain, and m/s for temperature, rainfall, and wind speed, respectively

extends to a larger precipitation value (Fig. 15c, d). Wind speed PDFs do not show any large changes (Figs. 15e, f, 16e, f).

The downscaled simulation results are very sensitive to topography. Precipitation is mainly caused by orographic lifting and mountain blocking. Therefore, model resolution must be high enough to depict topography correctly in order to produce good simulation results.

Previous studies on dynamical downscaling were mainly carried out with low-resolution simulations (e.g.,

40 km). Here, comparison of precipitation in January 2006 from GFS-PCM runs with different resolutions (i.e., domains) was made (Fig. 17) to evaluate the effect of model resolution on conclusions. Note that in this study, precipitation from a coarser resolution (e.g., domain 1) was obtained from upscaling results due to two-way interaction during the model integration. This may be slightly different from the use of a coarse resolution only (i.e., one-way nesting). Results showed that simulated precipitation strength and fine-scale features were highly

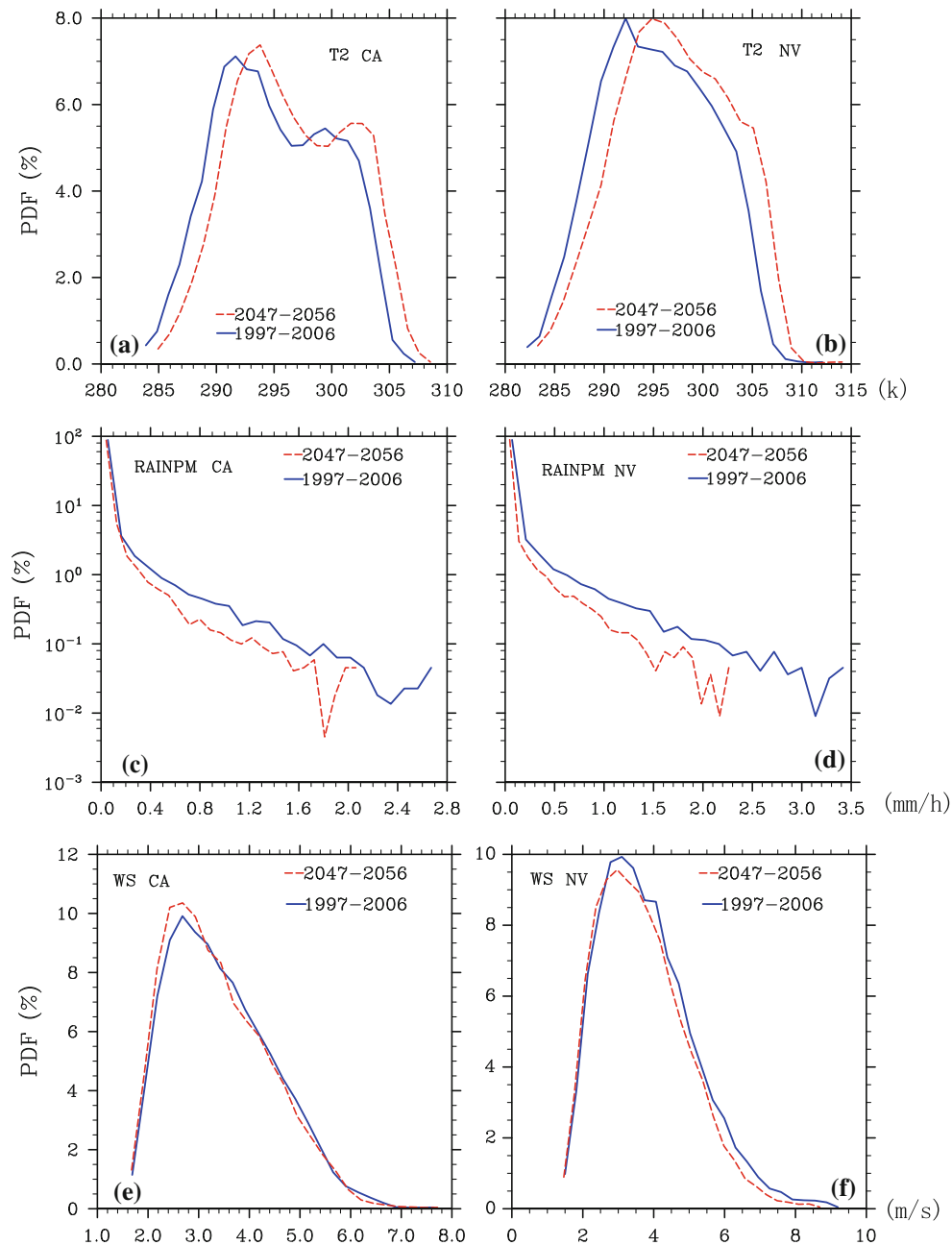


Fig. 16 Same as in Fig. 15 except for summer

dependent upon model resolution, especially in mountainous regions. The information from fine-scale features is very important to some regional-scale studies, such as of hydrological cycles in watersheds. Although there was a wet bias in southern CA from WRF-PCM runs, which can be contributed from both PCM and WRF simulations, the bias will be canceled in the difference field if the same bias is assumed for current and future PCM-WRF runs. Thus, the climate trend obtained in this study still provides some useful information.

5 Summary and conclusions

The possible influences of climate change on California were investigated with WRF dynamical downscaling on the outputs of PCM under the Business As Usual (BAU) scenario with a 4 km horizontal resolution. Current PCM-based dynamical downscaling results were compared with the dynamical downscaling from GFS inputs and PRISM statistically downscaled station data. Dominant features were consistent among WRF-PCM runs, WRF-GFS runs,

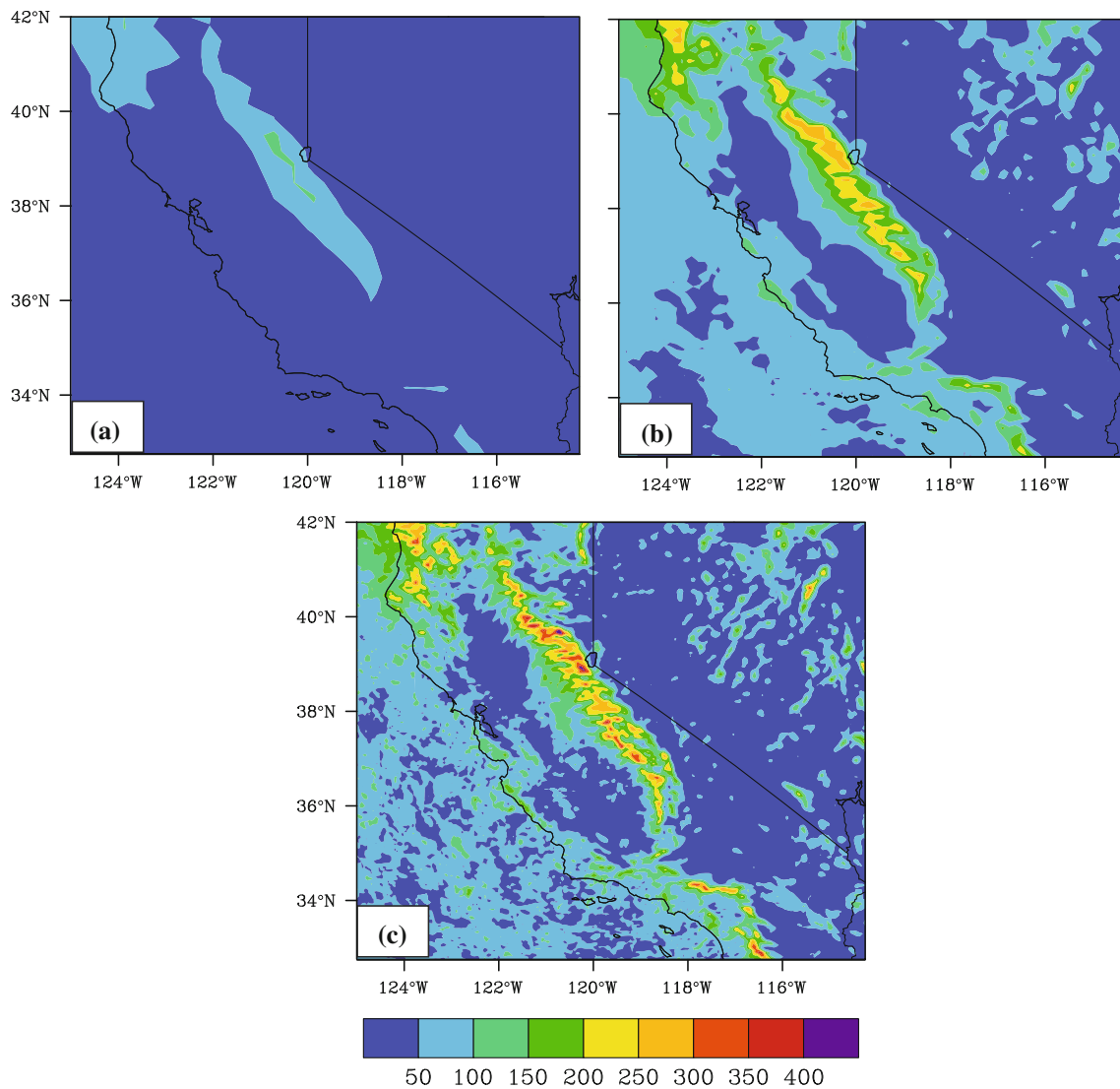


Fig. 17 Simulated January precipitation (mm/month) in 2006 from WRF-PCM runs for horizontal resolutions at **a** 36 km, **b** 12 km, and **c** 4 km

and PRISM. The statistical downscaling results have a tendency to estimate less variability in the parameter values, perhaps due to data sparseness resulting in a smoothing effect when compared with the dynamical downscaling, especially in the complex topographic region of California.

The possible influences of climate change on California and Nevada regions were investigated with both observational data analysis and model simulations. According to PRISM results, increasing precipitation was found in northern California by comparing current (1999–2008) and past (1979–1988) observational results. Comparisons between model current runs (1979–2006) and future runs (2047–2056) also suggested possible precipitation increases in California, especially in the north. Using the BAU scenario, the surface air temperature increases by 1–1.5°C (2–3°F) for California and 1.5–2°C (3–4°F) for Nevada. Winter precipitation is expected to increase in northern

California under a warming climate, but California becomes drier in the summer. The surface winds only change noticeably at higher elevations. Increasing surface air temperature leads to more winter precipitation falling as rain instead of snow, earlier snow melt, and more extreme events (heat waves, heavy precipitation, etc.). PRISM data suggest that the freezing level has already moved to higher elevations in the past 30 years. Model simulations also suggest a similar change in the future snowpack. More hot days in the Sacramento Valley and the southern part of California and Nevada are also expected. Rainfall frequency along the coastal region and the region from San Francisco inland are predicted to increase. Increasing temperature leads to an atmosphere that can hold more moisture, and provides more fuel for rain in the coastal region. However, increasing temperature also increases the height of the lifting condensation level, having a negative

effect on precipitation. The Coast Mountains block moisture at the coast, resulting in little change in rain frequency in the inland region. Heavy precipitation events occur in northern California and the southern Californian coast, which seems related to large scale forcing (e.g., cold front or tropical storm invasion). Predictions depend on the model resolution, and downscaling with a higher resolution may be needed for areas with complex topography.

It must be mentioned that our conclusions are solely based on downscaling results of one regional climate model (RCM) driven by the outputs of one global climate model (GCM) under the BAU emission scenario. It is expected that the use of different RCMs, GCMs and/or different emission scenarios might give different conclusions. Therefore, an ensemble approach, which uses combinations of different RCMs, GCMs, and emission scenarios with a longer downscaling time period, to estimate the uncertainties and the impacts of climate change on California is encouraged for future work when more computing resources are available.

Acknowledgments We thank Mary Tyree from the Scripps Institute of Oceanography at University of California, San Diego for her help on getting PCM data. This research is supported by NSF 0619139, Cyberinfrastructure for Environmental Observatories: Prototype Systems to Address Cross-Cutting Needs (CEO:P) initiative award, Coast-to-Mountain Environmental Transect (COMET). The PRISM dataset was downloaded from its website (<http://www.prism.oregonstate.edu/>). The supercomputational resources were supported by the National Typhoon and Flood Research Institute in Taiwan and the National Center for Atmospheric Research in the U.S.

Open Access This article is distributed under the terms of the Creative Commons Attribution Noncommercial License which permits any noncommercial use, distribution, and reproduction in any medium, provided the original author(s) and source are credited.

References

- Allan RP, Soden BJ (2008) Atmospheric warming and the amplification of precipitation extremes. *Science* 321:1481–1484
- Barnett T, Malone R, Pennell W, Stammer D, Semtner B, Washington W (2004) The effects of climate change on water resources in the west: introduction and overview. *Clim Change* 62:1–11
- Barnett TP, Pierce DW, Hidalgo HG, Bonfils C, Santer BD, Das T, Bala G, Wood AW, Nozawa T, Mirin AA, Cayan DR, Dettinger MD (2008) Human-induced changes in the hydrology of the western United States. *Science* 319:284–287
- Bell JL, Sloan LC, Snyder MA (2004) Regional changes in extreme climatic events: a future climate scenario. *J Clim* 17:81–87
- Caldwell P, Chin HNS, Bader DC, Bala G (2009) Evaluation of a WRF dynamical downscaling simulation over California. *Clim Change* 95:499–521
- Cayan DR (1996) Interannual climate variability and snowpack in the western United States. *J Clim* 9:928–948
- Cayan DR, Kammerdiener SA, Dettinger MD, Caprio JM, Peterson DH (2001) Changes in the onset of spring in the western United States. *Bull Am Meteorol Soc* 82:399–415
- Christensen OB, Christensen JH, Machenhauer B, Botzet M (1998) Very high-resolution regional climate simulations over Scandinavia—Present climate. *J Clim* 11:3204–3229
- Daly C, Neilson RP, Phillips DL (1994) A statistical-topographic model for mapping climatological precipitation over mountainous terrain. *J Appl Meteorol* 33:140–158
- DeGaetano AT, Allen RJ (2002) Trends in twentieth-century temperature extremes across the United States. *J Clim* 15:3188–3205
- Dettinger MD, Cayan DR (1995) Large-scale atmospheric forcing of recent trends toward early snowmelt runoff in California. *J Clim* 8:606–623
- Dettinger MD, Cayan DR, Meyer MK, Jeton AE (2004) Simulation hydrologic responses to climate variations and change in the Merced, Carson, and American river Basins, Sierra Nevada, California, 1900–2099. *Clim Change* 62:283–317
- DiLuzio M, Johnson GL, Daly C, Eischeid JK, Arnold JG (2008) Constructing retrospective gridded daily precipitation and temperature datasets for the conterminous United States. *J Appl Meteorol Clim* 47:475–497
- Dudhia J (1989) Numerical study of convection observed during the winter monsoon experiment using a mesoscale two-dimensional model. *J Atmos Sci* 46:3077–3107
- Easterling DR (2002) Recent changes in frost days and the frost-free season in the United States. *Bull Am Meteorol Soc* 83:1327–1332
- Easterling DR, Evans JL, Groisman PYa, Karl TR, Kunkel KE, Ambenje P (2000) Observed variability and trends in extreme climate events: a brief review. *Bull Am Meteorol Soc* 81:417–425
- Giorgi F, Shields C (1999) Tests of precipitation parameterizations available in latest version of NCAR regional climate model (RegCM) over continental United States. *J Geophys Res* 104D:6353–6375
- Grell GA, Devenyi D (2002) A generalized approach to parameterizing convection combining ensemble and data assimilation techniques. *Geophys Res Lett* 29(14). doi: [10.1029/2002GL015311](https://doi.org/10.1029/2002GL015311)
- Griffiths GM, Salinger MJ, Leleu I (2003) Trends in extreme daily rainfall in the South Pacific and relations to the South Pacific convergence zone. *Int J Climatol* 23:847–869
- Groisman PYa, Sherstyukov BG, Razuvaev VN, Knight RW, Enloe JG, Stroumentova NS, Whitfield PH, Førland E, Hannsen-Bauer I, Tuomenvirta H, Aleksandersson H, Mescherskaya AV, Karl TR (2007) Potential forest fire danger over northern Eurasia: changes during the 20th century. *Glob Planet Change* 46. doi: [10.1016/j.gloplacha.2006.07.029](https://doi.org/10.1016/j.gloplacha.2006.07.029)
- Groisman PYa, Knight RW, Karl TR (2001) Heavy precipitation and high streamflow in the contiguous United States: trends in the twentieth century. *Bull Am Meteorol Soc* 82:219–246
- Groisman PYa, Knight RW, Karl TR, Easterling DR, Sun B, Lawrimore JH (2004) Contemporary changes of the hydrological cycle over the contiguous United States: trends derived from in situ observations. *J Hydrometeorol* 5:64–85
- Groisman PYa, Knight RW, Easterling DR, Karl TR, Hegerl GC, Razuvaev VN (2005) Trends in intense precipitation in the climate record. *J Clim* 18:1326–1350
- Herath S, Ratnayake U (2004) Monitoring rainfall trends to predict adverse impacts—a case study from Sri Lanka (1964–1993). *Global Environ Change* 14:71–79
- Hong SY, Dudhia J, Chen SH (2004) A revised approach to ice microphysical processes for the bulk parameterization of cloud-sand precipitation. *Mon Weather Rev* 132:103–120
- Hong SY, Noh Y, Dudhia J (2006) A new vertical diffusion package with an explicit treatment of entrainment processes. *Mon Weather Rev* 134:2318–2341

- Huntington TG (2006) Evidence for intensification of the global water cycle: review and synthesis. *J Hydrol* 319:83–95
- Im ES, Jung IW, Chang H, Bae DH, Kwon WT (2009) Hydroclimatic response to dynamically downscaled climate change simulations for Korean basins. *Clim Change* 100:485–508. doi: [10.1007/s10584-009-9691-2](https://doi.org/10.1007/s10584-009-9691-2)
- Intergovernmental Panel on Climate Change (IPCC) (2007) Synthesis report, Contribution of Working Groups I, II and III to the Fourth Assessment Report of the Intergovernmental Panel on Climate Change Core Writing Team. In: Pachauri RK, Reisinger A (eds) IPCC, Geneva, Switzerland, pp 104. (http://www.ipcc.ch/publications_and_data/publications_ipcc_fourth_assessment_report_synthesis_report.htm)
- Jones RG, Murphy JM, Noguer M, King AB (1997) Simulation of climate change over Europe using a nested regional climate model. Comparison of driving and regional model responses to a doubling of carbon dioxide concentration. *Q J R Meteorol Soc* 123:265–292
- Joseph R, Nigam S (2006) ENSO evolution and teleconnections in IPCC's twentieth-century climate simulations: realistic representation? *J Clim* 19:4360–4377
- Kanamitsu M, Kanamaru H (2007) Fifty-seven-year California reanalysis downscaling at 10 km (CaRD10). Part I: system detail and validation with observations. *J Clim* 20:5553–5571
- Kendon EJ, Rowell DP, Jones RG, Buonomo E (2008) Robustness of future changes in local precipitation extremes. *J Clim* 21:4280–4297
- Kim J, Kim TK, Arritt RW, Miller NJ (2002) Impacts of increased atmospheric CO₂ on the hydroclimate of the Western United States. *J Clim* 15:1926–1942
- Knowles N, Dettinger MD, Cayan DR (2006) Trends in snowfall versus rainfall in the western United States. *J Clim* 19:4545–4559
- Kunkel KE et al (2003) Temporal variations of extreme precipitation events in the United States: 1895–2000. *Geophys Res Lett* 30:1900. doi: [10.1029/2003GL018052](https://doi.org/10.1029/2003GL018052)
- Leung LR, Ghan SJ (1999) Pacific Northwest climate sensitivity simulated by a regional climate model driven by a GCM. Part I: control simulations. *J Clim* 12:2010–2030
- Leung LR, Qian Y, Bian X, Washington WM, Han J, Roads J (2004) Mid-century ensemble regional climate change scenarios for the western United States. *Clim Change* 62:75–113
- Liu Y, Warner TT, Bowers JF, Carson LP, Chen F, Clough CA, Davis CA, Egeland CH, Halvorson SF, Huck TW Jr, Malone RE, Rife DL, Sheu R, Swerdlin SP, Weingarten DS (2008) The operational mesogamma-scale analysis and forecast system of the U.S. Army Test and Evaluation Command. Part 1: overview of the modeling system, the forecast products, and how the products are used. *J Appl Meteorol Clim* 47:1077–1092
- Manton MJ, Della-Marta PM, Haylock MR, Hennessy KJ, Nicholls N, Chambers LE, Collins DA, Daw G, Finet A, Gunawan D, Inape K, Isobe H, Kestin TS, Lefale P, Leyu CH, Lwin T, Maitrepierre L, Ouprasitwong N, Page CM, Pahalad J, Plummer N, Salinger MJ, Suppliah R, Tran VL, Trewin B, Tibig I, Yee D (2001) Trends in extreme daily rainfall and temperature in Southeast Asia and the South Pacific: 1961–1998. *Int J Climatol* 21:269–284
- Meehl GA, Hu A (2006) Mechanism for multi-decadal SST and precipitation variability in the Indo-Pacific region. *J Clim* 19:1605–1623
- Meehl GA, Tebaldi C (2004) More intense, more frequent, and longer lasting heat waves in the 21st century. *Science* 205:994–997
- Mlawer EJ, Taubman SJ, Brown PD, Iacono MJ, Clough SA (1997) Radiative transfer for inhomogeneous atmospheres: RRTM, a validated correlated-k model for the longwave. *J Geophys Res* 102:16663–16682
- Mote PW (2003) Trends in snow water equivalent in the Pacific Northwest and their climatic causes. *Geophys Res Lett* 30:1601. doi: [10.1029/2003GL017258](https://doi.org/10.1029/2003GL017258)
- Mote PW (2006) Climate-driven variability and trends in mountain snowpack in western North America. *J Clim* 19:6209–6220
- Mote PW, Salathé EP (2010) Future climate in the Pacific Northwest. *Clim Change*, doi: [10.1007/s10584-010-9848-z](https://doi.org/10.1007/s10584-010-9848-z)
- Mote PW, Hamlet AF, Clark MP, Lettenmaier DP (2005) Declining mountain snowpack in western North America. *Bull Am Meteorol Soc* 86:39–49
- NOAA's National Climatic Data Center (2008) The USHCN version 2 Serial Monthly Dataset. (<http://www.ncdc.noaa.gov/oa/climate/research/ushcn/>)
- Peterson TC et al (2002) Recent changes in climate extremes in the Caribbean region. *J Geophys Res* 107:4601. doi: [10.1029/2002JD002251](https://doi.org/10.1029/2002JD002251)
- Pierce DW, Barnett TP, Hidalgo HG, Das T, Bonfils C, Santer BD, Bala G, Dettinger MD, Cayan DR, Mirin A, Wood AW, Nozawa T (2008) Attribution of declining western U.S. snowpack to human effects. *J Clim* 21:6425–6444
- Rauscher SA, Pal JS, Diffenbaugh NS, Benedetti MM (2008) Future changes in snowmelt-driven runoff timing over the western US. *Geophys Res Lett* 35:L16703. doi: [10.1029/2008GL034424](https://doi.org/10.1029/2008GL034424)
- Robeson S (2004) Trends in time-varying percentiles of daily minimum and maximum temperature over North America. *Geophys Res Lett* 31:L04203. doi: [10.1029/2003GL019019](https://doi.org/10.1029/2003GL019019)
- Seager R, Ting M, Held I, Kushnir Y, Lu J, Vecchi G, Huang HP, Harnik N, Leetmaa A, Lau NC, Li C, Velez C, Naik N (2007) Model projections of an imminent transition to a more arid climate in southwestern North America. *Science* 316:1181. doi: [10.1126/science.1139601](https://doi.org/10.1126/science.1139601)
- Skamarock W, Klemp JB, Dudhia J, Gill DO, Barker DM, Wang W, Powers JG (2005) A description of the Advanced Research WRF version 2, NCAR Technical Note, NCAR/TN-468+STR
- Small EE, Giorgi F, Sloan LC (1999) Regional climate model simulation of precipitation in central Asia: mean and interannual variability. *J Geophys Res* 104D:6563–6582
- Snyder MA, Sloan LC, Bell JL (2004) Modeled regional climate change in the hydrologic regions of California: a CO₂ sensitivity study. *J Am Water Resour Assoc* 40:591–601
- Stewart I, Cayan DR, Dettinger MD (2004) Change in snowmelt runoff timing in western north America under a “Business as Usual” climate change Scenario. *Clim Change* 62:217–232
- Sun BM, Groisman PYa (2004) Variations in low cloud cover over the United States during the second half of the twentieth century. *J Clim* 17:1883–1888
- Trenberth KE, Jones PD, Ambenje P, Bojariu R, Easterling D, Klein Tank R, Parker D, Rahimzadeh R, Renwick JA, Rusticucci M, Soden B, Zhai P (2007) Observations: surface and atmospheric climate change. In: Solomon S, Qin D, Manning M, Chen Z, Marquis M, Averyt KB, Tignor M, Miller HL (eds) *Climate Change 2007: The Physical Science Basis*. Contribution of Working Group I to the Fourth Assessment Report of the Intergovernmental Panel on Climate Change. Cambridge University Press, Cambridge
- U. S. Global Change Research Program (2009) Global climate change impacts in the United States. In: Karl RT, Melillo JM, Peterson TC (eds) Cambridge University Press, New York. <http://www.globalchange.gov/publications/reports/scientific-assessments/us-impacts>
- Vanrheenen NT, Wood AW, Palmer RN, Lettenmaier DP (2004) Potential implications of PCM climate change scenarios for Sacramento-San Joaquin river basin hydrology and water resources. *Clim Change* 62:257–281
- Weare BC (2008) How will changes in global climate influence California? *Calif Agric* 63:59–66